

**Effects of mid- to upper-tropospheric water on microwave emission**

M. S. Johnston et al.

This discussion paper is/has been under review for the journal Atmospheric Measurement Techniques (AMT). Please refer to the corresponding final paper in AMT if available.

# Simulating the effects of mid- to upper-tropospheric clouds on microwave emissions in EC-Earth using COSP

M. S. Johnston<sup>1</sup>, G. Holl<sup>2</sup>, J. Hocking<sup>3</sup>, S. J. Cooper<sup>4</sup>, and D. Chen<sup>1</sup>

<sup>1</sup>Department of Earth Sciences, University of Gothenburg, Gothenburg, Sweden

<sup>2</sup>Department of Meteorology, University of Reading, Reading, UK

<sup>3</sup>Satellite Applications, Met Office, Fitzroy Road, Exeter, UK

<sup>4</sup>Department Atmospheric Sciences, University of Utah, Salt Lake City, Utah, USA

Received: 29 September 2015 – Accepted: 29 October 2015 – Published: 12 November 2015

Correspondence to: M. S. Johnston (shejo284@gmail.com)

Published by Copernicus Publications on behalf of the European Geosciences Union.

Title Page

Abstract

Introduction

Conclusions

References

Tables

Figures



Back

Close

Full Screen / Esc

Printer-friendly Version

Interactive Discussion



## Abstract

In this work, the Cloud Feedback Model Intercomparison (CFMIP) Observation Simulation Package (COSP) is expanded to include scattering and emission effects of clouds and precipitation at passive microwave frequencies. This represents an advancement over the official version of COSP (version 1.4.0) in which only clear-sky brightness temperatures are simulated. To highlight the potential utility of this new microwave simulator, COSP results generated using the climate model EC-Earth's version 3 atmosphere as input are compared with Microwave Humidity Sounder (MHS) channel (190.311 GHz) observations. Specifically, simulated seasonal brightness temperatures ( $T_B$ ) are contrasted with MHS observations for the period December 2005 to November 2006 to identify possible biases in EC-Earth's cloud and atmosphere fields.

The EC-Earth's atmosphere closely reproduces the microwave signature of many of the major large-scale and regional scale features of the atmosphere and surface. Moreover, greater than 60% of the simulated  $T_B$  are within 3K of the NOAA-18 observations. However, COSP is unable to simulate sufficiently low  $T_B$  in areas of frequent deep convection. Within the Tropics, the model's atmosphere can yield an underestimation of  $T_B$  by nearly 30K for cloudy areas in the ITCZ. Possible reasons for this discrepancy include both incorrect amount of cloud ice water in the model simulations and incorrect ice particle scattering assumptions used in the COSP microwave forward model. These multiple sources of error highlight the non-unique nature of the simulated satellite measurements, a problem exacerbated by the fact that EC-Earth lacks detailed micro-physical parameters necessary for accurate forward model calculations. Such issues limit the robustness of our evaluation and suggest a general note of caution when making COSP-satellite observation evaluations.

# AMTD

8, 11753–11777, 2015

## Effects of mid- to upper-tropospheric water on microwave emission

M. S. Johnston et al.

Title Page

Abstract

Introduction

Conclusions

References

Tables

Figures



Back

Close

Full Screen / Esc

Printer-friendly Version

Interactive Discussion



## 1 Introduction

Clouds are an important factor in the planet's climate system because they interact with the incoming shortwave and outgoing longwave radiation. Their precise impact on the Earth's radiative budget depends upon both their micro-physical properties (e.g. cloud particle phase, size and shape) and macro-physical properties (e.g. geographical and temporal distributions). Furthermore, clouds and precipitation provide heating to the atmosphere through diabatic processes such as latent heat release. These cloud effects, in turn, interact with dynamics, convection, and water vapour in feedbacks that impact both weather and climate scale processes (see, for example Twomey, 1991; Wielicki et al., 1995; Stephens, 2005, and references therein).

Despite decades of climate modelling, simulated clouds have remained a persistent source of uncertainty in climate projections, as documented in International Panel on Climate Change (IPCC) Assessment Reports (2007 and 2013). Improved evaluation techniques for cloud representation are critical for reducing these model uncertainties (Randall et al., 2007). Simulated clouds are generally a function of both the large-scale and the convection schemes of climate and Numerical Weather Prediction (NWP) models. These two schemes are often strongly interlinked, which makes it difficult to pinpoint sources of error arising from model parameterizations and assumptions. Similarly, the constraint of model cloud and precipitation fields with satellite-derived observations is problematic, due to differences in how quantities are defined and due to large uncertainties associated with operational products.

The COSP (Cloud Feedback Model Intercomparison Project (CFMIP) Observation Simulation Package) was developed to help facilitate model-to-observation comparisons. By creating a simulated cloud product that is based on a model's atmosphere but using a forward model similar to the one used to generate the observational product, COSP allows a meaningful and consistent evaluation approach. Furthermore, the COSP explicitly accounts for spatial discrepancies associated with the footprints of satellite observations and model cloud field (Bodas-Salcedo et al., 2009, 2011).

# AMTD

8, 11753–11777, 2015

## Effects of mid- to upper-tropospheric water on microwave emission

M. S. Johnston et al.

Title Page

Abstract

Introduction

Conclusions

References

Tables

Figures



Back

Close

Full Screen / Esc

Printer-friendly Version

Interactive Discussion









scattering information. Activating this interface requires information regarding clouds and atmospheric hydrometeors to be passed from the model, thus the COSP interface is expanded to simulate passive microwave sensors in all-sky conditions.

The information passed from EC-Earth to RTTOV includes the profiles of temperature, land–sea mask, effective cloud fraction, cloud liquid water and ice, sea ice fraction, atmospheric pressure, precipitating water and ice, and specific humidity. Surface emissivity is provided by the fast microwave emissivity model version 5 (FASTEM-5 Bormann et al., 2012) over ocean and TELSEM (Tool to Estimate Land Surface Emissivities at Microwave frequencies) (Aires et al., 2011) over land. The land surface emissivity is derived from monthly-mean climatology of emissivities generated from microwave observations operating at frequencies below 100 GHz. These values are then interpolated for single channel emissivities at 190.311 GHz. Over water, FASTEM-5 emissivity calculations are based on surface winds, salinity, and sea surface temperature. The sea-ice parameters used with FASTEM in this study are the default set given in English and Hewison (1998, Table 1).

In order to simulate the microwave scattering and absorption effects of atmospheric hydrometers, RTTOV employs the delta-Eddington approximation (Bauer et al., 2006) technique. This technique allows high speed and accurate calculations of monochromatic fluxes through the atmosphere (Joseph et al., 1976). Moreover, RTTOV uses a cloud overlap assumption, which is described in Geer et al. (2009).

All-sky brightness temperatures are calculated in two steps: first, the clear-sky  $T_B$  profiles are calculated followed by another set of calculations that include scattering effects from atmospheric constituents. The clear-sky and scattering brightness temperatures are then linearly combined using Eq. (1) to give a total brightness temperature  $T_B^{\text{Total}}$ .

$$T_B^{\text{Total}} = (1 - C)T_B^{\text{Clear}} + CT_B^{\text{Hydrometeor}}, \quad (1)$$

## Effects of mid- to upper-tropospheric water on microwave emission

M. S. Johnston et al.

Title Page

Abstract

Introduction

Conclusions

References

Tables

Figures

◀

▶

◀

▶

Back

Close

Full Screen / Esc

Printer-friendly Version

Interactive Discussion







## Effects of mid- to upper-tropospheric water on microwave emission

M. S. Johnston et al.

Title Page

Abstract

Introduction

Conclusions

References

Tables

Figures

◀

▶

◀

▶

Back

Close

Full Screen / Esc

Printer-friendly Version

Interactive Discussion



together nadir and off-nadir measurements therefore results in average radiances that are difficult to interpret. To prevent this, but still get sufficient measurements per grid cell and month, we consider MHS radiances at scan angles of at most  $\pm 5^\circ$  off-nadir. Secondly, we collected all incidents where the criterion in Eq. (2) is fulfilled. Here, we applied the same nadir angle criterion as when calculating the gridded mean  $T_B$ .

In the Tropics large areas of clouds and intense precipitation are often associated with deep convective activity. To establish this fact, we identify areas of deep convection using a method developed by Hong et al. (2005). This method employs a combination of the differences between channels 3, 4 and 5 to create an inequality test given in Eq. (2). The inequality is satisfied only in areas of deep convection where the cloud top  $T_B$  represents a local minimum,

$$\Delta T_{35} \geq \Delta T_{34} \geq \Delta T_{45} > 0, \quad (2)$$

where  $\Delta T_{xy}$  is difference in  $T_B$  between channels  $x$  and  $y$ .

### 3.2 COSP-RTTOV data quality filtering

Microwave radiative transfer calculations may be complicated by surface emissivity issues associated with certain surface types. For example, sea ice and snow covered surfaces may have great variability in surface emission under different conditions which in turn may translate to large uncertainties in the simulated  $T_B$ . These uncertainties can be reduced using seasonal averages, although substantial biases may still remain. Well-known problem areas are filtered out from the simulation according to Geer et al. (2014, Table 3), thus enabling a fairer comparison with the NOAA-18 observations. The filtering criteria that have been adapted for this study are listed in Table 1. The simulated data were filtered at each time step before being compiled into monthly averages.

## 4 Results

This work primarily focuses on the effects of cloud and precipitation condensates in the Tropics on passive microwave emission at 190.311 GHz. However, we also briefly present the results poleward of  $\pm 30^\circ$  where the effects of atmospheric water becomes harder to disentangle from surface contamination. Figure 1 depicts the seasonal mean  $T_B$  calculated from RTTOV using the EC-Earth atmosphere (left column) and observed by NOAA-18 (right column) for December 2005 to November 2006. The time period is divided into four seasons: DJF (a, b), MAM (c, d), JJA (e, f), and SON (g, h).

The NOAA-18 observations show top of the atmosphere 190.311 GHz microwave  $T_B$  associated with the Earth's large scale general circulation features. The values range from near 280K in the Tropics to 250K over the poles. The ITCZ is clearly seen inside the Tropics as characterised by a band of reduced  $T_B$  with values typically near 260 to 270K. Finer scale features such as snow-covered Greenland and Antarctica and the Arctic, with its transition from ice to open water, are easily discerned in NOAA-18 seasonal data.

RTTOV generated  $T_B$  using EC-Earth atmosphere as input agree well to the first order with NOAA-18 observations. The overall range of  $T_B$  are similar, however, the model tends to be a bit warmer than NOAA-18 as evidenced by the broad areas with  $T_B$  around unit 280 K in the Tropics. The model develops a well-defined ITCZ, although it tends to be narrower in area and warmer than the NOAA-18 observations. Features poleward of  $\pm 30^\circ$  are also captured by the model to the first order. For example, the Arctic shows significant warming in the JJA season, which is consistent with melting of the sea ice during the Boreal summer months. Finally, areas of high elevation such as the Andes, northern Rockies, Tibetan Plateau, and Himalayas tend to show similar results for both EC-Earth and NOAA-18. However, perfect agreement is not expected. Large uncertainties in assumed surface emissivity for these high-latitude and high-elevation areas will result in correspondingly large uncertainties in the simulated  $T_B$ .

## Effects of mid- to upper-tropospheric water on microwave emission

M. S. Johnston et al.

Title Page

Abstract

Introduction

Conclusions

References

Tables

Figures



Back

Close

Full Screen / Esc

Printer-friendly Version

Interactive Discussion



The NOAA-18 results suggest the presence of broad areas of lower  $T_B$  ( $\lesssim 268$  K) for all seasons within the ITCZ. These areas of low  $T_B$  are non-contiguous, patchy and occur over both land and ocean. Such disparities are not seen over regions of subsidence, i.e. generally cloud-free areas.

In order to investigate the aforementioned patches of lower  $T_B$  within the ITCZ in an objective manner, we applied Eq. (2) to the NOAA-18 radiances prior to building the seasonal means. In order to match the instantaneous results from the inequality to statistical means, we assume no deep convection occurs poleward of  $60^\circ$ , which left 3080 possible cases of deep convection for the month of July 2005. We later choose a region ( $-20$  to  $30^\circ$  latitude and  $60$  to  $180^\circ$  E longitude) and a  $T_B$  of  $268$  K, which closely matches the edge of the ITCZ. Of the possible 1001 cases of deep convective events, 747 or ( $\approx 75\%$ ) fall within region selected (not shown). The results strongly suggests that the patchy areas of lower  $T_B$  are largely collocated with the areas of deep convection.

Figure 2 quantifies  $T_B^{\text{EC-EARTH}} - T_B^{\text{NOAA-18}} = \Delta T_B$ . We limit the colour range of the figure to about twice the standard deviation ( $\sim 5$  K) of  $\Delta T_B$  within the Tropics for better resolution at small values. Unfiltered and filtered model data are presented in the left and right panels, respectively. As above, unfiltered  $\Delta T_B$  ( $\Delta T_B^{\text{UF}}$ ) includes areas where there are large uncertainties in the simulated results due to assumed surface emissivity, e.g. snow or sea ice conditions. The filtered  $\Delta T_B$  ( $\Delta T_B^{\text{F}}$ ) data, by removing low confidence values according to Table 1, allows us to better focus on the impact of clouds and precipitation.

The results show that the spread in  $\Delta T_B^{\text{UF}}$  can reach  $\sim \pm 10$  K, and locally up to  $\sim \pm 40$  K (not shown) for all seasons. The ITCZ consistently contains regions of positive  $\Delta T_B$ , suggesting a systematic bias in the model's atmosphere when calculating  $T_B$  in areas of convective clouds. Despite the clear bias in the ITCZ, the figures show many regions with a  $\Delta T_B$  within  $\approx \pm 3$  K.

Table 2 provides a statistical description of Fig. 2. The table presents the mean and standard deviation of  $\Delta T_B$  as well as the percentage of grid boxes where  $|\Delta T_B| \leq 3$  K.

## Effects of mid- to upper-tropospheric water on microwave emission

M. S. Johnston et al.

Title Page

Abstract

Introduction

Conclusions

References

Tables

Figures

◀

▶

◀

▶

Back

Close

Full Screen / Esc

Printer-friendly Version

Interactive Discussion





## 5 Discussion and conclusions

In this study, the satellite simulator COSP is upgraded to include clouds and precipitation in its calculations of microwave radiances. This represents an advancement over the official version of COSP (version 1.4.0) in which only clear-sky brightness temperatures are simulated. The calculations associated with hydrometeor scattering and emission are accomplished modifying of the RTTOV forward model interface used for the clear-sky conditions in the COSP simulator.

Microwave radiances generated from COSP, assuming an EC-Earth atmosphere, were compared with MHS (190.311 GHz) observations for the year 2006 at the global scale. By focusing on seasonal time scales, we minimise any bias in our analyses caused by spatio-temporal errors in the modelled clouds and precipitation fields. Clear-sky calculations are omitted from the study.

The results (Figs. 1–4) show good agreement between microwave brightness temperatures as simulated using the EC-Earth atmosphere and those observed from NOAA-18 for some key atmospheric features, e.g. ITCZ and areas of large-scale subsidence. However, there are regions with clear large biases whose signs (positive/negative) are seasonally dependent (for example western North America). These regions of large biases are known problematic issues when conducting  $T_B$  calculations above certain surface types. These regions of the simulated  $T_B$  were filtered according to Table 1, and affected mostly the high latitudes of the Northern Hemisphere. For subsidence areas with generally low cloud frequency, the model atmosphere shows a lower  $T_B$  than NOAA-18, possibly indicating too little surface or water vapour emission in the simulated radiances.

In most cases where clouds are present, the model tends to overestimate the  $T_B$ . For deep convective regions within the ITCZ with significant ice cloud and precipitation aloft, observed zonal MHS  $T_B$  are 3K greater than corresponding COSP simulated values. Locally, this difference can be much higher ( $\sim 30$ K). This discrepancy could occur if EC-Earth has either too little ice aloft or if the assumed cloud and hydrometeor

## Effects of mid- to upper-tropospheric water on microwave emission

M. S. Johnston et al.

Title Page

Abstract

Introduction

Conclusions

References

Tables

Figures



Back

Close

Full Screen / Esc

Printer-friendly Version

Interactive Discussion







## Effects of mid- to upper-tropospheric water on microwave emission

M. S. Johnston et al.

Title Page

Abstract

Introduction

Conclusions

References

Tables

Figures



Back

Close

Full Screen / Esc

Printer-friendly Version

Interactive Discussion



- Bauer, P., Geer, A. J., Lopez, P., and Salmond, D.: Direct 4D-Var assimilation of all-sky radiances. Part I: Implementation, *Q. J. R. Meteorol. Soc.*, 136, 1868–1885, 2010. 11756
- Bodas-Salcedo, A., Webb, M. J., Brooks, M. E., Ringer, M. A., Williams, K. D., Milton, S. F., and Wilson, D. R.: Evaluating cloud systems in the met office global forecast model using simulated CloudSat radar reflectivities, *J. Geophys. Res.: Atmos.*, 114, 1–18, doi:10.1029/2007JD009620, 2009. 11755
- Bodas-Salcedo, A., Webb, M. J., Bony, S., Chepfer, H., Dufresne, J. L., Klein, S. A., Zhang, Y., Marchand, R., Haynes, J. M., Pincus, R., and John, V. O.: COSP: Satellite simulation software for model assessment, *B. Am. Meteorol. Soc.*, 92, 1023–1043, doi:10.1175/2011BAMS2856.1, 2011. 11755
- Bonsignori, R.: The microwave humidity sounder MHS in-orbit performance assessment – art. no. 67440A, in: *Sensors, Systems, and Next-Generation Satellites XI*, edited by: Meynart, R., Neeck, S. P., Shimoda, H., and Habib, S., vol. 6744 of *Proceedings of the Society of Photo-Optical Instrumentation Engineers (SPIE)*, p. A7440, SPIE-INT SOC OPTICAL ENGINEERING, 1000 20TH ST, PO BOX 10, BELLINGHAM, WA 98227-0010 USA, Conference on Sensors, Systems, and Next-Generation Satellites XI, Florence, Italy, 17–20 September 2007. 11756
- Bormann, N., Geer, A., and English, S.: Evaluation of the Microwave Ocean Surface Emissivity Model FASTEM-5 in the IFS, Technical Memorandum 667, European Centre for Medium-Range Weather Forecasts, Reading, England, 2012. 11759
- Buehler, S., Eriksson, P., Kuhn, T., von Engeln, A., and Verdes, C.: ARTS, the atmospheric radiative transfer simulator, *J. Quant. Spectrosc. Ra.*, 91, 65–93, doi:10.1016/j.jqsrt.2004.05.051, 2005. 11761
- Dee, D. P., Uppala, S. M., Simmons, A. J., Berrisford, P., Poli, P., Kobayashi, S., Andrae, U., Balmaseda, M. A., Balsamo, G., Bauer, P., Bechtold, P., Beljaars, A. C. M., van de Berg, L., Bidlot, J., Bormann, N., Delsol, C., Dragani, R., Fuentes, M., Geer, A. J., Haimberger, L., Healy, S. B., Hersbach, H., Hólm, E. V., Isaksen, L., Kållberg, P., Köhler, M., Matricardi, M., McNally, A. P., Monge-Sanz, B. M., Morcrette, J. J., Park, B. K., Peubey, C., de Rosnay, P., Tavolato, C., Thépaut, J. N., and Vitart, F.: The ERA-Interim reanalysis: configuration and performance of the data assimilation system, *Q. J. R. Meteorol. Soc.*, 137, 553–597, doi:10.1002/qj.828, 2011. 11757



## Effects of mid- to upper-tropospheric water on microwave emission

M. S. Johnston et al.

Title Page

Abstract

Introduction

Conclusions

References

Tables

Figures



Back

Close

Full Screen / Esc

Printer-friendly Version

Interactive Discussion



- Joseph, J. H., Wiscombe, W. J., and Weinman, J. A.: The Delta-Eddington Approximation for Radiative Flux Transfer, *J. Atmos. Sci.*, 33, 2452–2459, doi:10.1175/1520-0469(1976)033<2452:TDEAFR>2.0.CO;2, 1976. 11759
- 5 Klein, S. A., Zhang, Y., Zelinka, M. D., Pincus, R., Boyle, J., and Gleckler, P. J.: Are climate model simulations of clouds improving? An evaluation using the ISCCP simulator, *J. Geophys. Res.: Atmos.*, 118, 1329–1342, doi:10.1002/jgrd.50141, 2013. 11756
- Marshall, J. S. and Palmer, W. M. K.: The distribution of raindrops with size, *J. Meteor.*, 5, 165–166, 1948. 11760
- 10 Nam, C., Bony, S., Dufresne, J. L., and Chepfer, H.: The too few, too bright tropical low-cloud problem in CMIP5 models, *Geophys. Res. Lett.*, 39, 1–7, doi:10.1029/2012GL053421, 2012. 11756
- Nam, C. C. W. and Quaas, J.: Evaluation of clouds and precipitation in the ECHAM5 general circulation model using CALIPSO and cloudsat satellite data, *J. Clim.*, 25, 4975–4992, doi:10.1175/JCLI-D-11-00347.1, 2012. 11756
- 15 Randall, D. A., Wood, R. A., Bony, S., Colman, R., Fichet, T., Fyfe, J., Kattsov, V., Pitman, A., Shukla, J., Srinivasan, J., Stouffer, R. J., Sumi, A., and Taylor, K. E.: Climate models and their evaluation, in: *Climate Change 2007: The physical science basis. Contribution of Working Group I to the Fourth Assessment Report of the IPCC (FAR)*, University Press, Cambridge, United Kingdom and New York, NY, USA, 589–662, 2007. 11755
- 20 Saunders, R., Hewison, T., Stringer, S., and Atkinson, N.: The radiometric characterization of AMSU-B, *IEEE T. Microw. Theory*, 43, 760–771, 1995. 11760
- Saunders, R., Matricardi, M., and Brunel, P.: An improved fast radiative transfer model for assimilation of satellite radiance observations, *Q. J. R. Meteorol. Soc.*, 125, 1407–1425, 1999. 11758
- 25 Stephens, G. L.: Cloud feedbacks in the climate system: a critical review, *J. Clim.*, 18, 237–273, 2005. 11755
- Twomey, S.: Aerosols, clouds and radiation, *Atmos. Environ. A*, 25, 2435–2442, doi:10.1016/0960-1686(91)90159-5, 1991. 11755
- Wielicki, B., Cess, R., King, M., Randall, D., and Harrison, E.: Mission to planet Earth – Role of clouds and radiation in climate, *B. Am. Meteorol. Soc.*, 76, 2125–2153, 1995. 11755
- 30 Yurkin, M. A., Maltsev, V. P., and Hoekstra, A. G.: The discrete dipole approximation for simulation of light scattering by particles much larger than the wavelength, *J. Quant. Spectrosc. Radiat. Transfer*, 106, 546–557, doi:10.1016/j.jqsrt.2007.01.033, 2007. 11760

## Effects of mid- to upper-tropospheric water on microwave emission

M. S. Johnston et al.

Title Page

Abstract

Introduction

Conclusions

References

Tables

Figures



Back

Close

Full Screen / Esc

Printer-friendly Version

Interactive Discussion



**Table 1.** List of the data quality criteria used to filter the COSP simulation. (Adapted from Geer et al., 2014, Table 3).

Latitude poleward of $\pm 60^\circ$
Orography greater than 800 m
Fractional land–sea mask (0.2 – 0.8)
A sea-ice fraction greater than 0
Over ocean, surface temperatures $< 274$ K
Snow-covered land areas

## Effects of mid- to upper-tropospheric water on microwave emission

M. S. Johnston et al.

Title Page

Abstract

Introduction

Conclusions

References

Tables

Figures

◀

▶

◀

▶

Back

Close

Full Screen / Esc

Printer-friendly Version

Interactive Discussion



**Table 2.** Table of the average, standard deviation, and the percentage of grid boxes where the difference  $T_B^{\text{EC-EARTH}} - T_B^{\text{NOAA-18}}$  is greater is within a reasonable uncertainty assumption of 3K. Statistics taken over the globally and the Tropics for the unfiltered and filtered data. The filtered data are given in parentheses.

Season	Mean		SD		$ \Delta T_B  \leq 3$	
	Global [K]	Tropics [K]	Global [K]	Tropics [K]	Global [%]	Tropics [%]
DJF	1.7 (1.9)	2.0 (1.9)	5.2 (3.2)	3.1 (3.0)	62.2 (70.8)	67.1 (68.7)
MAM	2.4 (2.0)	2.2 (2.1)	5.1 (2.7)	3.0 (2.9)	59.4 (69.4)	73.2 (65.1)
JJA	1.9 (1.8)	2.1 (2.1)	4.6 (2.6)	3.1 (3.0)	68.3 (73.7)	66.5 (68.2)
SON	1.5 (1.9)	2.4 (2.3)	4.3 (2.7)	3.0 (2.9)	63.6 (72.3)	63.6 (66.0)

## Effects of mid- to upper-tropospheric water on microwave emission

M. S. Johnston et al.

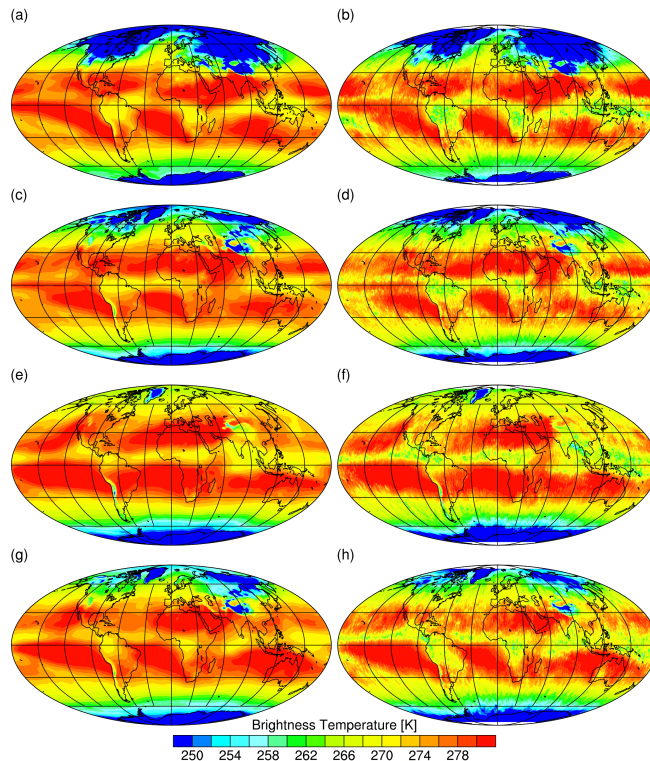


**Figure 1.** Seasonal (December 2005 to November 2006) satellite-derived mean  $T_B$ , expressed in Kelvin, at 190.311 GHz, simulated using COSP (left column: **a**, **c**, **e**, and **g**) and NOAA18 MHS sensor (right column: **b**, **d**, **f**, and **h**). The seasons are displayed as follows: DJF: (**a**, **b**), MAM: (**c**, **d**), JJA: (**e**, **f**), and SON: (**g**, **h**).

[Title Page](#)[Abstract](#)[Introduction](#)[Conclusions](#)[References](#)[Tables](#)[Figures](#)[◀](#)[▶](#)[◀](#)[▶](#)[Back](#)[Close](#)[Full Screen / Esc](#)[Printer-friendly Version](#)[Interactive Discussion](#)

## Effects of mid- to upper-tropospheric water on microwave emission

M. S. Johnston et al.

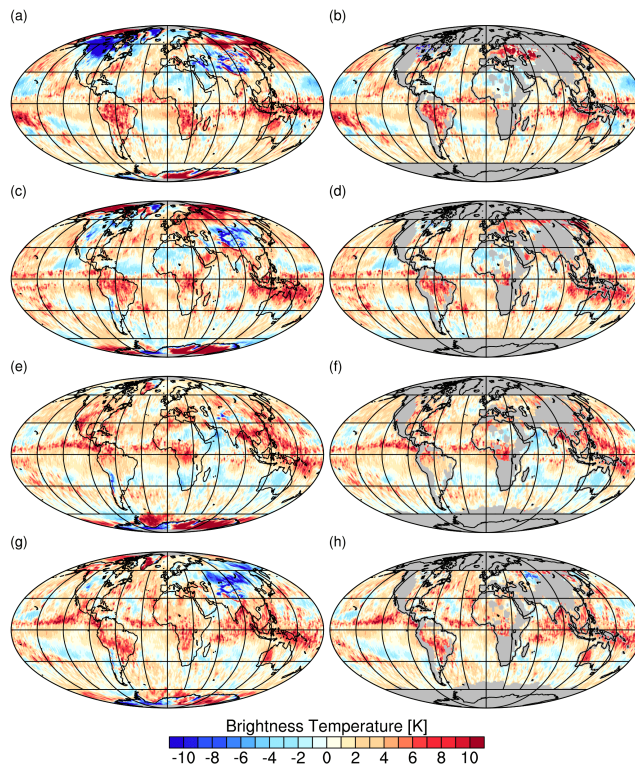


**Figure 2.** 2006 difference ( $T_B^{\text{EC-EARTH}} - T_B^{\text{NOAA-18}} = \Delta T_B$ ) in seasonal satellite-derived mean  $T_B$ , expressed in Kelvin, at 190.311 GHz, simulated using COSP-RTTOV MHS simulator. The column on the left depicts the differences without filtering, while the right column shows the differences filtered according to Table 1. The seasons are in each row as: DJF: (a, b), MAM: (c, d), JJA: (e, f), and SON: (g, h). The filtered areas are depicted as gray.

## Effects of mid- to upper-tropospheric water on microwave emission

M. S. Johnston et al.

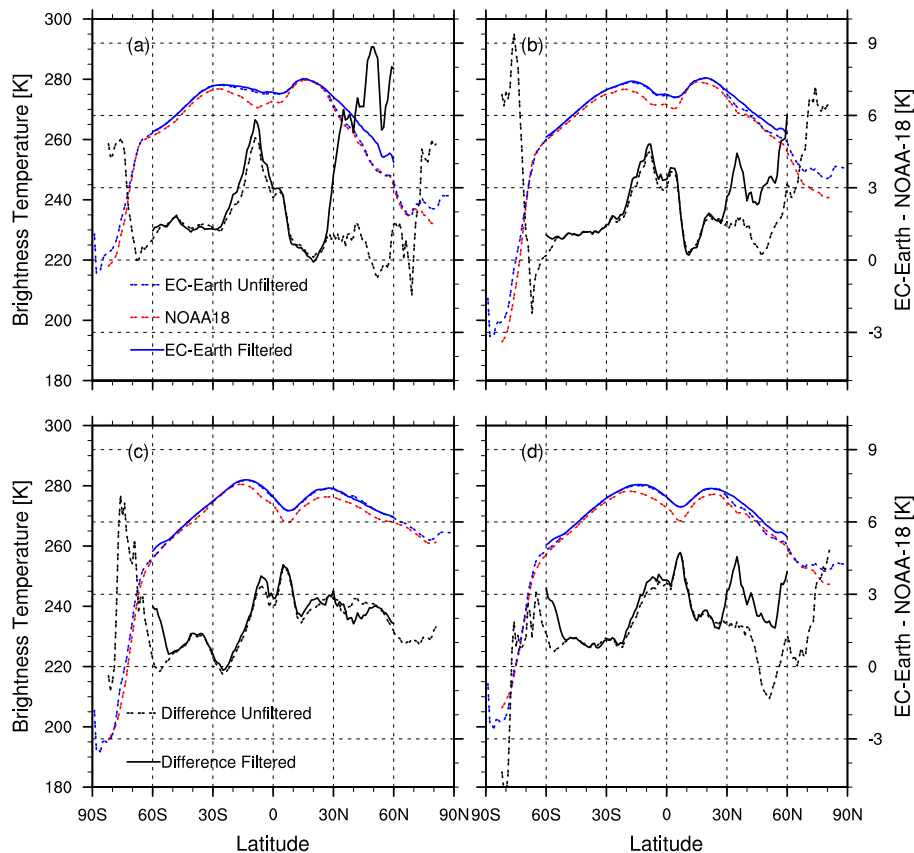


**Figure 3.** Seasonal zonal mean  $T_B$  for channel 5 (190.311 GHz) of the NOAA-18 MHS sensor (red) and EC-Earth-COSP simulated (blue). The black line shows the zonal mean of  $\Delta T_B^{UF}$ . The data for the filtered case are depicted by solid lines. DJF represented by (a) MAM by (b), JJA by (c), and SON by (d).

Title Page

Abstract

Introduction

Conclusions

References

Tables

Figures

◀

▶

◀

▶

Back

Close

Full Screen / Esc

Printer-friendly Version

Interactive Discussion



## Effects of mid- to upper-tropospheric water on microwave emission

M. S. Johnston et al.

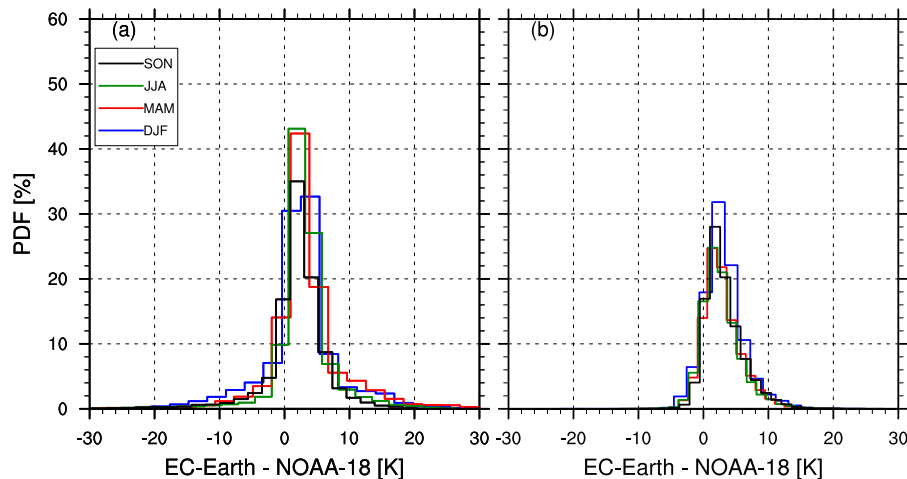


**Figure 4.** Probability density function of  $\Delta T_B^{UF}$  for channel 5 (190.311 GHz). Plot (a) depicts the differences poleward of  $\pm 30$  latitude and plot (b) between  $\pm 30$  latitude. Note: plots shows a shortened X-axis in order to increase focus on the centre the plot.

Title Page

Abstract

Introduction

Conclusions

References

Tables

Figures

◀

▶

◀

▶

Back

Close

Full Screen / Esc

Printer-friendly Version

Interactive Discussion

